Quasi-linear Theory of Wind-Wave Generation Applied to Wave Forecasting

PETER A. E. M. JANSSEN

Department of Oceanography, Royal Netherlands Meteorological Institute (KNMI), De Bilt, The Netherlands

(Manuscript received 6 August 1990, in final form 29 April 1991)

ABSTRACT

The effect of wind-generated gravity waves on the airflow is discussed using quasi-linear theory of wind-wave generation. In this theory, both the effects of the waves and the effect of air turbulence on the mean wave profile are taken into account.

The main result of this theory is that for young wind sea most of the stress in the boundary layer is determined by momentum transfer from wind to waves, therefore, resulting in a strong interaction between wind and waves. For old wind sea there is, however, hardly any coupling. As a consequence, a sensitive dependence of the aerodynamic drag on wave age is found, explaining the scatter in plots of the experimentally observed drag as a function of the wind speed at 10-m height. Also, the growth rate of waves by wind is found to depend on wave age.

All this suggests that a proper description of the physics of the momentum transfer at the air–sea interface can only be given by coupling an atmospheric (boundary-layer) model with an ocean-wave prediction model. Here, results are presented of the coupling of a simple surface-layer model with a third-generation wave model. First, results obtained with a single gridpoint coupled model are discussed, and the evolution in time of wave height, wave stress, and the aerodynamic drag is investigated. Next, results obtained from a hindcast with the coupled model on the North Sea are discussed.

In both cases, the wave-induced stress is found to have some impact on the results for wave height, while the impact on the stress in the surface layer is significant.

1. Introduction

There is increasing interest in the simulation of the earth's climate by means of coupled ocean–atmosphere models. First attempts toward direct coupling reveal, however, basic shortcomings in our knowledge of air–sea fluxes. This is nicely illustrated by Cubasch (1989) where coupling of an atmospheric model (European Centre for Medium Range Weather Forecast model with spectral resolution of T21 and 16 levels) with the ocean model of Maier-Raimer et al. (1982) showed a definite trend in the mean atmospheric temperature. On the other hand, application of the flux correction method of Sausen et al. (1988) removes this drift in the climate.

In this paper, the problem of the interaction of wind and ocean waves is addressed. One reason is that knowledge of the sea state might improve our estimates of the momentum flux at the air–sea interface, as the wave-induced stress is a considerable fraction of the total stress within the surface layer (Komen 1985; Janssen 1989). This is especially true for young wind sea. A better knowledge of the momentum flux may result in improved estimates of heat and moisture fluxes, which play a key role in the evolution of a depression. This improved knowledge might also be beneficial for wave prediction, storm surge prediction, and the ocean circulation.

The plan of this paper is as follows: In section 2, a two-dimensional model for the generation of waves by wind in which the shape of the wind profile is determined by both turbulent fluxes and the wave-induced stress is briefly introduced. However, as in Miles (1957), it is assumed that the effect of turbulence on the wave-induced air motion may be neglected. Janssen (1989) solved a one-dimensional version of these quasi-linear equations on the computer and was able to determine the dependence of aerodynamic drag on the state of the sea waves. This approach, however, is not very practical when coupling an atmospheric model with a wave model, since, even on the Cray XMP48, it takes 60 seconds to compute the drag coefficient. An analytical approximation of the effect of ocean waves on the wind profile is, therefore, clearly desirable and is presented in this section.

From quasi-linear theory it is found that, in agreement with the observations of Donelan (1982), the aerodynamic drag over ocean waves depends on the sea state. A similar conclusion may be reached from the work of Jacobs (1989) who, however, only calculated the roughness length of airflow over old wind sea. A proper description of the momentum transfer from air to ocean (waves) can therefore only be given by coupling an atmospheric (boundary-layer) model with

Corresponding author address: Dr. Peter Janssen, KNMI, P.O. Box 201, 3730 AE De Bilt, The Netherlands.

a wave prediction model. Here, results of the coupling of a simple surface-layer model with the third-generation wave prediction model WAM (WAMDIG 1988) are discussed. In section 3, results obtained with a single gridpoint version of the coupled model are studied, and the evolution in time of wave height, wave stress, and aerodynamic drag is investigated. Especially in the initial stages of growth, a strong interaction between wind and waves is found, resulting in a substantial increase of the stress in the surface layer. Section 3 is also devoted to a discussion of results obtained from a hindcast with the coupled model on a limited area of the North Sea. In particular, the relation between aerodynamic drag and wind speed is emphasized to show that from the coupled model results a realistic scatter around the mean is found, similar to the in situ observations of Donelan (1982). Section 4 gives a summary of conclusions.

A preliminary account of this work was presented at the Royal Society discussion meeting on the dynamics of coupled atmosphere and ocean held on 13 and 14 December 1988 (Janssen et al. 1989). The present work differs in several respects, especially regarding the more realistic parameterizations of the effect of waves on wind and on the results of the aerodynamic drag.

2. Two-dimensional theory of wind-generated water waves

The purpose of this section is to introduce a simple parameterization of the quasi-linear theory of wind generation so that it can be applied to, for example, wave forecasting or climate modeling.

Before we do this it should be realized, however, that quasi-linear theory, which is based on Miles' resonance mechanism, has only restricted validity since, for high-frequency waves, effects of viscosity and air turbulence on the critical layer have not been taken into account. Nevertheless, realistic results are obtained, provided the energy loss to the short gravity–capillary waves is modeled by means of a roughness length, for example, the Charnock (1955) relation.

In Janssen (1982) and Janssen et al. (1989) only propagation of waves in one direction was considered. Therefore, the extension of quasi-linear theory to two dimensions will be presented in this paper first. We therefore consider the case where the wind $\vec{U}_0$ is blowing at an angle ϕ with the x axis. The wavenumber spectrum Φ then depends on both wavenumber k and direction θ. In principle, the equation for the wind profile must be treated as genuinely two-dimensional, since the total wave momentum may be pointed in a different direction than the wind. In practice, however, the wave stress is always in the wind direction because most of the wave stress is carried by the high-frequency waves, which respond rather quickly to a change in wind direction. From the outset, we therefore assume that the wave stress is in the wind direction so that only one component of the momentum equation for air has to be considered.

The theory becomes more transparent in a frame that has the x axis along the wind speed. Performing the rotation

$$x = x' \cos\theta - y' \sin\theta$$
$$y = y' \cos\theta - x' \sin\theta, \tag{1}$$

the momentum equation becomes

$$\frac{\partial}{\partial t} U_0 = D_w \frac{\partial^2}{\partial z^2} U_0 + \frac{\partial}{\partial z} \tau_{\text{turb}} + \frac{\partial}{\partial z} \tau_{\text{visc}}, \tag{2}$$

where z denotes the height from the mean water surface. Here, τ_{turb} is the turbulent stress, which is modeled by a mixing length hypothesis,

$$\tau_{\text{turb}} = l^2 \left| \frac{\partial}{\partial z} U_0 \right| \frac{\partial}{\partial z} U_0, \tag{3}$$

where $U_0(z)$ is the wind profile and the mixing length l is given by $l = \kappa z$ (κ is the von Kármán constant).

The viscous stress is given by the usual expression

$$\tau_{\text{visc}} = \nu_a \frac{\partial}{\partial z} U_0, \tag{4}$$

where ν_a is the kinematic viscosity of air.

The wave diffusion coefficient D_w depends on the wavenumber spectrum Φ and is given by

$$D_w = \pi \int d\theta \frac{\omega^2 k}{|c - v_g|} |\chi|^2 \Phi(k, \theta) \cos^2\theta. \tag{5}$$

Here, $\omega = \sqrt{gk}$, g is the acceleration due to gravity, c the phase speed ω/k, v_g the group velocity $\partial\omega/\partial k$, and χ the normalized vertical component of the wave-induced velocity in air. In the expression for D_w, wavenumber and angular frequency are eliminated in favor of z, using the resonance condition

$$W = U_0(z) - c/\cos\theta = 0. \tag{6}$$

The effect of waves on the wind is similar to the effect of molecular viscosity, and for negative curvature there is a transfer of momentum from air to the ocean waves. In that event, the airflow over surface gravity waves experiences, compared to air flow over a flat plate, an additional stress that has been termed the wave-induced stress τ_w (Janssen 1989). In the steady state, the momentum balance (2) may be integrated once with respect to height to obtain

$$\tau_w + \tau_{\text{turb}} + \tau_{\text{visc}} = \tau, \tag{7}$$

where the total stress $\tau = u_*^2$ with u_* the friction velocity, and the wave-induced stress is then given by

$$\tau_w(z) = -\int_z^\infty dz D_w \frac{\partial^2}{\partial z^2} U_0. \tag{8}$$

The loss of momentum from the airflow must, by conservation of momentum, be accompanied by a growth of the water waves. The corresponding growth rate γ of the waves by wind is, according to Miles (1957), given by

$$\gamma = -\pi\epsilon c|\chi_c|^2 \frac{U''_{0c}}{|U'_{0c}|}, \tag{9}$$

where ϵ is the air–sea density ratio, and the subscript c refers to evaluation at the critical height $z = z_c$, as defined by Eq. (6). Here, the wave-induced velocity χ obeys the Rayleigh equation

$$W\left(\frac{\partial^2}{\partial z^2} - k^2\right)\chi = W''\chi, \tag{10}$$

subject to the boundary conditions

$$\chi(0) = 1, \quad \chi(\infty) \to 0.$$

It should be noted that a wave propagating under an angle θ with respect to the wind only interacts with its effective component $U_0 \cos\theta$. In other words, the growth of a wave propagating at an angle θ can be obtained from the growth rate of a wave propagating in the wind direction by replacing U_0 by $U_0 \cos\theta$. Following scaling arguments of Miles (1957), the growth rate of the waves by wind can then be written as

$$\gamma = \epsilon\beta\omega\left(\frac{u_*}{c}\right)^2 \cos^2\theta. \tag{11}$$

The so-called Miles parameter β depends, in general, on three dimensionless quantities,

$$\beta = \beta\{u_* \cos\theta/c, s, \Omega\}, \tag{12}$$

where s is the wave steepness, $s = k^4\phi$, and $\Omega = gz_0/u_*^2$, with z_0 a typical roughness length of the wind profile.

For unidirectional propagation, Janssen (1989) solved the nonlinear set of Eqs. (3)–(10) by means of an iteration procedure. The main result was that the aerodynamic drag over sea waves was found to depend on the sea state; young wind sea resulted in higher drag than old wind sea. This result is in good agreement with observations by Donelan (1982) and HEXOS (Maat et al. 1991).

For practical applications, such as the coupling of a weather prediction model with the WAM model (WAMDI 1988), the iteration procedure is too time consuming. Even the unidirectional problem takes 60 seconds on the Cray XMP-48. In the remainder of this section, an analytical approximation will therefore be discussed.

a. Analytical approximation to the growth rate γ

Observations of the growth of waves by wind and the linear Miles theory [$s \to 0$ in (12)] show a u_*/c dependence of the growth rate that, for high-frequency waves, is not in agreement with the well-known Snyder et al. (1981) parameterization. This is clearly shown in Fig. 1. Thus, according to Eq. (11) the relative growth rate γ/ω scales as $(u_*/c)^2$, as for relatively high-frequency waves β becomes a constant. The Snyder et al. parameterization would give a linear dependence, resulting in a considerable underestimation of wind input for high-frequency waves and therefore an underestimation of the wave-induced stress.

Finite amplitude waves, however, will give rise to a finite wave diffusion coefficient D_w and might therefore affect the curvature in the wind profile in such a way that the growth of the waves is reduced. This is especially true for the high-frequency waves that have their critical layer just above the wave surface. As a result, a rougher flow is obtained with larger roughness length. Hence, as the critical height is proportional to the roughness length, the growth rate of the longer waves will depend on the momentum transfer from air to the short, high-frequency waves.

Miles (1965) determined the effect of the short waves on the growth of wind waves by assuming that the growth rate γ/ω is mainly determined by the curvature

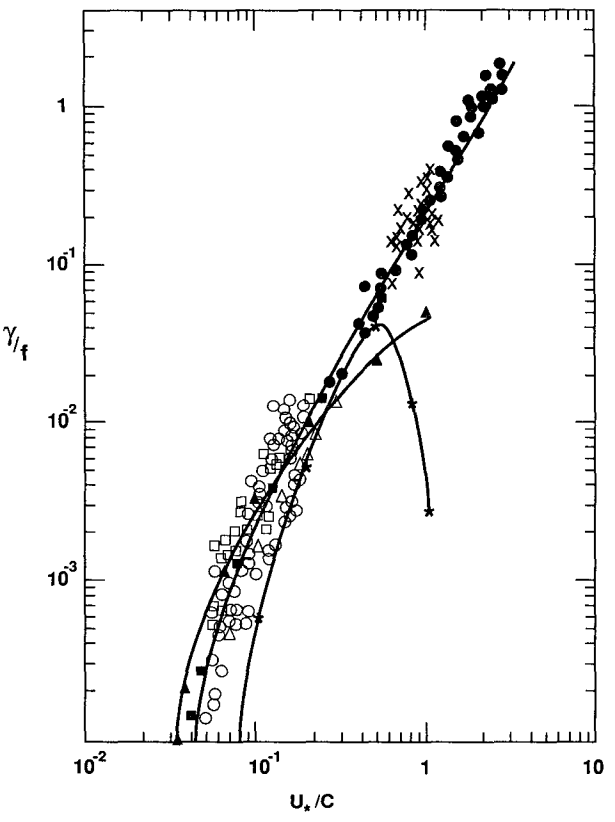

FIG. 1. Dimensionless growth rate γ/f as a function of u^*/c according to observations compiled by Plant (1982). Full line (——) is linear Miles theory, with Charnock constant $\alpha_{CH} = 0.0144$. The symbol △ is Snyder et al.'s (1981) parameterization, □ is (22) with $\alpha_{CH} = 0.0144$, and * is (22) with $\alpha_{CH} = 0.144$.

in the wind profile. As a result, only the growth of the high-frequency waves is found to depend on the sea state, contrasting with the numerical results of Janssen (1989) who found that the growth of both high- and low-frequency waves depends on the sea state. The reason for this discrepancy is that Miles did not realize that the critical height of the longer waves will increase by a significant amount because in the presence of high-frequency waves the airflow becomes rougher.

We therefore consider the dependence of the growth rate (through the critical height) on the state of the high-frequency waves. Fortunately, we know from the numerical results of Janssen (1989) that, even in case of young wind sea when the effect of the waves on the wind profile is strong, the wind profile still has a logarithmic shape, although with different roughness length. If the effect of gravity–capillary waves is modeled by means of the well-known Charnock relation,

$$z_0 = \alpha u_*^2/g, \quad \alpha = \text{const}, \tag{13}$$

and the effect of the (short) gravity waves by means of a roughness length z_1, then the wind profile that satisfies the boundary condition $U_0(z_0) = 0$ is given by

$$U_0(z) = \frac{u_*}{\kappa} \ln\left(\frac{z + z_1}{z_0 + z_1}\right). \tag{14}$$

Determining the roughness length z_1 from the drag coefficient, as calculated by Janssen (1989), gives excellent agreement between Eq. (14) and the numerical results for the wind profile, as may be inferred from Fig. 2. Also, Jacobs (1989) found that the effect of waves on a turbulent airflow may be represented by an effective roughness length.

The observation that the wind profile may be described by the logarithmic profile (14) considerably simplifies the problem of the parameterizing the growth of waves by wind. The result is that the Miles parameter depends on only two dimensionless parameters

$$\beta = \beta(u_* \cos\theta/c, \Omega).$$

Miles (1957) obtained for the logarithmic profile (14) an approximate expression for the parameter β. He found that β depends only on the dimensionless critical height, μ,

$$\mu \equiv k(z_c + z_1), \tag{15}$$

which, using the wind profile (14), may be written as

$$\mu = \left(\frac{u_*}{\kappa c}\right)^2 \Omega e^{\kappa c/u_* \cos\theta}, \tag{16}$$

where Ω is the so-called profile parameter

$$\Omega = g(z_0 + z_1)\kappa^2/u_*^2. \tag{17}$$

For fixed friction velocity the effect of the waves on the growth rate is just represented by Ω through its dependence on z_1. Unfortunately, when compared with the numerical solution of the Rayleigh equation (10), Miles' approximate expression for β is too large by a factor of 3. Based on Miles' work, we found, however, after some trial and error that the expression

$$\beta = \frac{1.2}{\kappa^2} \mu \ln^4\mu, \quad \mu \leqslant 1 \tag{18}$$

compares favorably with the numerical results (see Fig. 1).

To summarize our discussion, the growth rate of waves by wind is given by

$$\frac{\gamma}{\omega} = \epsilon\beta\left(\frac{u_*}{c}\right)^2 \cos^2\theta, \tag{19}$$

where β is given by (18), and μ and Ω are given by (16)–(17).

In Fig. 1 the relative growth rate γ/f (where f is frequency $\omega/2\pi$), according to (19), has been compared with experimental data for the case in which the effect of the waves on the wind is disregarded ($z_1 \to 0$). The roughness length z_0 is given by the Charnock relation, with Charnock constant $\alpha = 0.0144$. This gives a profile parameter $\Omega = 2.410^{-3}$. Agreement with laboratory data ($u_*/c > 0.2$) and the field data of Snyder et al. ($u_*/c < 0;.2$) is good in view of a number of uncertainties regarding both this theory and the experimental data. Quasi-linear theory neglects the effects of air turbulence on the wave-induced airflow (e.g., see Jacobs 1987), which is not justified for high-frequency waves, while for low-frequency waves effects of gustiness may be important (Nikolayeva and Tsimring 1986). On the other hand, the experimental data may also be questioned to some extent. The field data of Snyder et al. (1981) are based on a direct measurement of wind input by measuring the correlation between the time derivative of the surface elevation and the

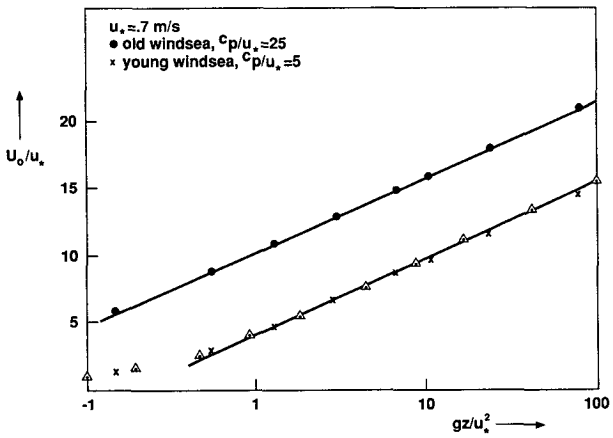

FIG. 2. Effect of waves on wind profile according to Janssen (1989). ● old wind sea ($c_p/u_* = 25$), × is the young wind sea ($c_p/u_* = 5$), and △ denotes the parameterization (14) for young wind sea.

pressure. The pressure signal, however, is obtained at a fixed height and is then extrapolated to the surface using potential theory. This may give an overestimate of the growth rate (Makin 1988). Finally, the laboratory data of Plant and Wright (1977) are obtained from the time evolution of the surface elevation and can therefore, strictly speaking, not be regarded as an independent measurement of wind input, since, for example, nonlinear interactions are important as well (Janssen 1987).

In general, knowledge of the effect of waves on the wind, e.g., the wave roughness length z_1, is required. The determination of z_1 from the wind speed at 10-m height and the wave stress will be discussed in the next subsection. It should be noted that the feedback effect of the waves on the growth by wind may be quite significant. This is shown in Fig. 1 where the dimensionless growth rate is plotted for a profile parameter Ω which is 10 times as large as the one with $z_1 = 0$. We remark that the experimental data are obtained for a much smoother flow.

b. *Dependence of total stress on wave stress and wind speed*

We now address the problem of the determination of total stress τ when the wave stress τ_w and the wind speed U_{10} at the 10-m height are given. Consider therefore the stress balance of airflow over ocean waves in the steady state, Eq. (7), and apply it at $z = z_0$. Neglecting viscous stress, the result is

$$\tau_w(z = z_0) + \tau_{\text{turb}}(z = z_0) = \tau. \tag{20}$$

With τ_{turb} given by (3) and using the logarithmic wind profile (14), the turbulent stress at $z = z_0$ is found to be

$$\tau_{\text{turb}}(z_0) = \tau\left(\frac{z_0}{z_0 + z_1}\right)^2. \tag{21}$$

The combination of (20) and (21) gives

$$z_1 = z_0\left(\frac{1}{\sqrt{1 - x}} - 1\right), \quad x = \tau_w/\tau$$

for z_1, and for $L \gg z_1$, the drag coefficient, defined as $C_D(L) = (u_*/U_0(L))^2$, becomes

$$C_D(z = L) = \left(\frac{\kappa}{\ln(L/z_2)}\right)^2, \quad z_2 = z_0/\sqrt{1 - x}. \tag{22}$$

Since $\tau = C_D U_0^2$, the total stress in the surface layer is obtained from an iterative solution of

$$\tau = \left\{\frac{\kappa U_0(L)}{\ln(L/z_2)}\right\}^2, \tag{23}$$

where we take L as 10 m. Therefore, for given wave stress τ_w and wind speed $U_0(10)$, we can determine the total stress τ and the roughness length z_2. What remains is a determination of the wave-induced stress τ_w, which will be done in the next subsection.

c. *The wave-induced stress τ_w*

Using conservation of momentum, the wave-induced stress $\tau_w(z = 0)$ may be related to the rate of change of wave momentum due to wind (Janssen 1989). Here the wave momentum $\vec{P}$ is given by

$$\vec{P} = \rho_w \omega \Phi(\vec{k})\vec{l}, \quad \vec{l} = \vec{k}/k. \tag{24}$$

Thus, the total wave-induced stress $\tau_w(0)$ is

$$\vec{\tau}_w(0) = \int k dk d\theta \frac{\partial}{\partial t}\vec{P}\Big|_{\text{wind}}. \tag{25}$$

With the help of the expression for the growth rate, Eq. (11), the total stress $\vec{\tau}_w$ may be written as

$$\vec{\tau}_w = \tau \int_0^\infty k dk \int_D d\theta k^2 \beta \Phi \cos^2\theta \vec{l},$$

$$D = |\theta| < \pi/2. \tag{26}$$

In the WAM model (WAMDI Group 1988), the energy-balance equation is solved in a finite-frequency range only. However, waves with a wavenumber higher than the cutoff value k_c will also contribute to the stress exerted on the airflow. We therefore divide the wave stress $\vec{\tau}_w$ into two parts,

$$\vec{\tau}_w = \vec{\tau}_{w,lf} + \vec{\tau}_{w,hf} \tag{27}$$

where

$$\vec{\tau}_{w,lf} = \tau \int_0^{k_c} k dk \int_D d\theta k^2 \beta \Phi \cos^2\theta \vec{l}$$

is determined by the dynamics of the model, while

$$\vec{\tau}_{w,hf} = \tau \int_{k_c}^\infty k dk \int_D d\theta k^2 \beta \Phi \cos^2\theta \vec{l}$$

will be parameterized by assuming a simple spectrum at high wavenumbers.

Because observations seem to favor a k^{-4} power law (Birch and Ewing 1986; Forristal 1981; Banner 1990), we decided to use this power law for the high wavenumber part of the spectrum, where the directional distribution is determined by the spectral energy at the highest resolved wavenumber $k = k_c$. With

$$\Phi(k, \theta) = \left(\frac{k_c}{k}\right)^4 \Phi(k_c, \theta), \tag{28}$$

the wave stress corresponding to the high wavenumber part of the spectrum becomes

$$\vec{\tau}_{whf} = \tau k_c^4 \int_{k_c}^\infty d\theta dk \frac{\beta}{k} \Phi(k_c, \theta) \cos^2\theta \vec{l}. \tag{29}$$

Since for these high wavenumbers β is virtually independent of direction, the high-frequency stress may be approximated by

$$\tau_{whf} = \tau k_c^4 \int_D d\theta \cos^2 \vec{l}\,\Phi(k_c, \theta) \int_{k_c}^{\infty} dk \frac{\beta}{k}, \quad (30)$$

where the integrals over both θ and k are evaluated numerically.

In this respect, it should be remarked that, if β is a constant over the whole wavenumber range (an approximation advocated by Plant and Wright), then the integral over wavenumber would give rise to a logarithmic singularity. Our parameterization of the Miles parameter β, Eq. (18), gives a finite answer for the high-frequency stress because β vanishes for $\mu = k(z_0 + z_1) = 1$. Obviously, the rougher the airflow, the smaller the wavenumber range over which the high-frequency wave stress is evaluated. This is easily understood in the framework of quasi-linear theory since, as soon as the wave stress becomes substantial, the waves will modify the airflow in such a way that the transfer of momentum from air to water waves is quenched (Janssen 1982; Janssen 1989). A reduction of the momentum transfer is achieved by reducing the curvature in the wind profile [cf. (9)]; hence, the air flow becomes rougher.

3. The coupled ocean-wave–atmosphere model

A considerable fraction of the stress in the atmospheric boundary-layer model is carried by ocean waves, especially for young wind sea. In Janssen (1989), it was found that the aerodynamic drag is a sensitive function of the sea state, where the wave spectrum was given by the JONSWAP shape (JONSWAP 1973), with a Phillips constant α_p depending sensitively on the age of the wind sea, which is measured by the ratio c_p/u_* (with c_p the phase speed of the peak).

An important question is what happens when the wave spectrum is allowed to evolve according to the dynamics of the energy balance equation. Do we still obtain a sensitive dependence of aerodynamic drag on the wave age? This question is important because, if the drag is more or less independent of the sea state, coupling of an atmospheric boundary-layer model with an ocean-wave model would be meaningless, despite the fact that the wave-induced stress is a considerable fraction of the total stress. Seen from the viewpoint of atmospheric modelers, a simple parameterization of the wave-induced stress would suffice. However, the careful observations of Donelan (1982) and Maat et al. (1991) show a considerable dependence of the aerodynamic drag on sea state, suggesting that coupling of an atmospheric boundary-layer model and a wave model is indeed meaningful. Therefore, the results of our coupling experiment should give a sensitive wave-age dependence of the drag over ocean waves.

The boundary-layer equation used here takes only the effects of turbulent and wave-induced stress on the momentum balance into account. Integrating over a layer with thickness Δz_i where i denotes the ith layer, we have

$$\frac{\partial}{\partial t} \vec{U}_i = \frac{\vec{\tau}_{i+1} - \vec{\tau}_i}{\Delta z_i}, \quad (31)$$

where $\vec{U}_i$ is the average wind speed and, away from the surface ($i \geq 1$), the stress $\vec{\tau}_i$ is given by

$$\vec{\tau}_i = K_i(\Delta \vec{U}_i / \Delta z_i), \quad (32)$$

where $\Delta \vec{U}_i = \vec{U}_i - \vec{U}_{i-1}$, $K_i = l_i^2 |\Delta \vec{U}_i / \Delta z_i|$, and l_i is the mixing length $l_i = \kappa z_i$ with κ the von Kármán constant. At the surface ($i = 0$) the stress is given by

$$\vec{\tau}_0 = C_D |\vec{U}_0| \vec{U}_0, \quad (33)$$

where $C_D = C_D(U_0, \tau_w)$ is given by Eq. (22).

In the coupling experiment it was assumed that the wind field relaxes almost instantaneously to its equilibrium. This is a reasonable assumption, since a typical relaxation time scale T for the surface layer is given by $T \approx l_0/u_* < 1$ min for $l_0 \approx 20$ m and $u_* \approx 0.5 - 1$ m s^{-1}, whereas a typical time scale for the wave field is of the order of 15 min. From the condition of constant stress, one then finds the following relation between the wind speed at the top of the boundary layer, U_N, and the surface wind speed U_0:

$$U_0 = U_N - \tau_0^{1/2} \sum_{i=1}^{N} \Delta z_i / l_i, \quad (34)$$

where τ_0 is given by Eq. (33). Thus, for given wind speed U_N and wave stress τ_w, (33)–(34) can be solved for U_0 and τ_0 by means of iteration.

Let us now turn to the determination of the wave stress τ_w. In terms of the frequency spectrum $F(f, \theta)$, defined through the relation $Fdfd\theta = \Phi k dk d\theta$, the low-frequency part of the wave stress τ_{wlf} is given by

$$\tau_{wlf} = \frac{1}{\epsilon} \int_0^{f_c} \int_D df d\theta \omega \vec{l} \left. \frac{\partial F}{\partial t} \right|_{\text{wind}}, \quad l = \vec{k}/k, \quad (35)$$

where $f_c = \sqrt{gk_c}/2\pi$ and the high-frequency part of the wave stress is determined by Eq. (30). The evolution of the two-dimensional frequency spectrum $F(f, \theta)$ is determined by the energy balance equation (WAMDI Group 1988)

$$\frac{\partial}{\partial t} F + \vec{v}_g \cdot \frac{\partial}{\partial x} F = S = S_{in} + S_{nl} + S_{ds}, \quad (36)$$

where $\vec{v}_g$ is the group velocity, $\partial\omega/\partial\vec{k}$, and the source terms describe the physics of the generation of surface waves by the wind (S_{in}), nonlinear interactions (S_{nl}), and dissipation due to whitecapping. The nonlinear interactions are determined by means of the discrete interaction approximation (S. Hasselmann et al. 1985). The wind input term is, according to our results of the previous section, a function of both the dimensionless

phase speed c/u_* and the sea state, which is related to the roughness length of the airflow. Recall that young wind sea with large steepness will result in a rough flow and old wind sea in a much smoother flow. The wind input term S_{in} is therefore given by

$$S_{in} = \gamma F, \tag{37}$$

with γ as in Eq. (19). The dissipation source function is linear in the wave spectrum with a coefficient that depends on the wave energy E, mean wavenumber $\langle k \rangle$, and mean angular frequency $\langle \omega \rangle$,

$$S_{ds} = -\beta \langle \omega \rangle (\langle k \rangle^2 E)^2 (k/\langle k \rangle)^m F, \tag{38}$$

where E is the total wave variance

$$E = \int df d\theta F,$$

and $\langle k \rangle$ and $\langle \omega \rangle$ are averages with the spectrum F as weight (cf., WAMDI Group 1988). The standard WAM model has $\beta = 2.6$ and $m = 1$. As discussed in Janssen et al. (1989), the choice $m = 1$ leads to unsatisfactory behavior of the high-frequency tail of the spectrum; especially for old wind sea, the energy in the high frequencies was too large, giving a too large Phillips constant and a too large wave-induced stress. In the coupling experiment, we therefore decided to choose $m = 2$ with $\beta = 2.6$. The consequence is a stronger dissipation of the high-frequency waves but a weaker dissipation for low frequencies. It should be noted that the dissipation due to whitecapping in the standard WAM model (hence $m = 1$) is based on Hasselmann (1974). In this theory, it is argued that whitecapping is a process that is weak in the mean; therefore, the corresponding dissipation source term is linear in the wave spectrum. Assuming that there is a large separation between the length scale of the waves and the whitecaps, the power m of the wavenumber in the dissipation source function is found to be equal to 1. However, for the high-frequency part of the wave spectrum, such a large gap between waves and whitecaps may not exist, allowing the possibility of a different dependence of the dissipation on wavenumber.

The energy balance equation (36) is solved for F in a finite frequency domain D only. This domain is defined by

$$D: 0.0418 < f < \min(f_c, 0.4114), \tag{39}$$

where f_c is given by the maximum of $2.5\langle \omega \rangle / 2\pi$ and $4f_{PM}$, with f_{PM} the Pierson–Moskovitch frequency. For frequencies larger than f_c, we assume an f^{-5} tail where the directional distribution is determined by the one at $f = f_c$. Wave energy, mean wavenumber, and mean frequency are then determined by an integration over the full frequency range, whereas the contribution of the wave-induced stress τ_w corresponding to $f > f_c$ is given by Eq. (30).

We performed numerical experiments with a one gridpoint version of this coupled wave-surface layer model, implemented on a personal computer (AT with coprocessor). Therefore, we only report results of wave height, Phillips constant α_p, wave stress, and drag coefficient on duration, displayed in Figs. 3, 4, 5, and 6. The initial condition was a JONSWAP spectrum with peak frequency $f_p = 0.27$ Hz, Phillips constant $\alpha_p = 0.025$, overshoot parameter $\gamma = 3.0$, and spectral width $\sigma = 0.1$. The directional distribution was given by the usual $\cos^2$ distribution. The energy balance equation was integrated for 12 directions and 25 frequencies (on a logarithmic scale, 0.0418–0.4114), using an implicit scheme (WAMDI Group 1988). The integration time step was 3 minutes, whereas wind and waves were coupled every 15 min so that there was sufficient time for the wind to relax to a new equilibrium. We varied the number of layers, but present only results for a single layer as results were qualitatively similar. In addition, this makes a comparison with results from the North Sea hindcast possible. The wind speed, U_N at 10-m height, was chosen to be $U_N = 18.45$ m s^{-1}, corresponding, in the absence of waves, to a friction velocity of $u_* = 0.85$ m s^{-1} (with Charnock constant $\alpha = 0.0185$). The first experiment was a reference run with the wave model without any coupling between wind and waves. This was achieved by simply disregarding the effect of waves on the roughness length [cf. Eq. (22)]. The Charnock constant was chosen to be $\alpha = 0.0185$. The corresponding results in Figs. 3, 4, and 5 are denoted by the plus (+) symbol.

Next, the wave model was coupled with our steady-state one-layer model of the surface. The effect of waves on the roughness length was taken into account through Eq. (22). As for older wind sea the wave-induced stress still has a finite value, so the Charnock constant, was, by trial and error, given the lower value $\alpha = 0.0110$. This choice for α gives old wind sea the same roughness

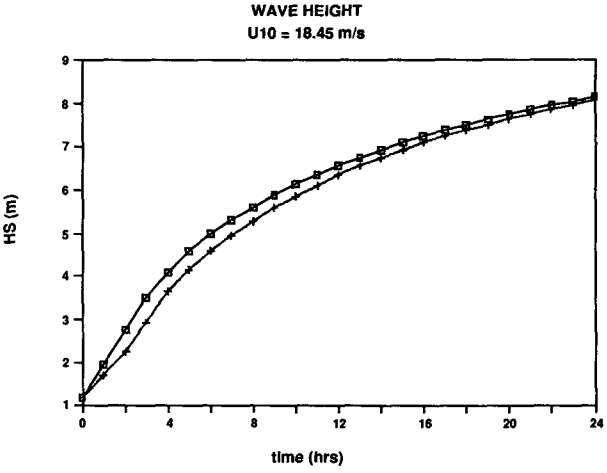

FIG. 3. Wave height against time for coupled-wave, surface-layer model (□), and uncoupled wave model (+).

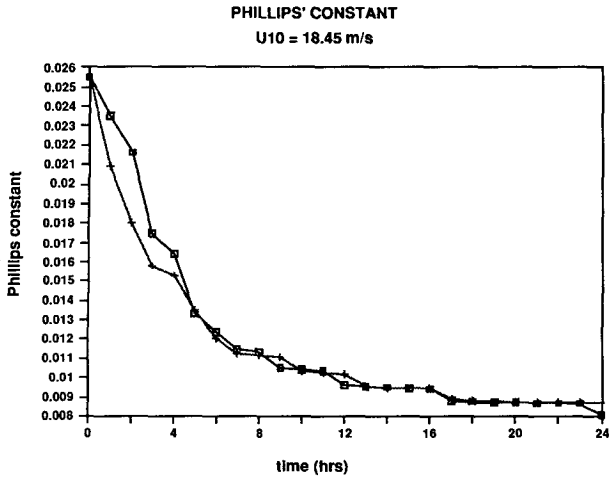

FIG. 4. Phillips' constant as a function of time for uncoupled model (+) and coupled model (□).

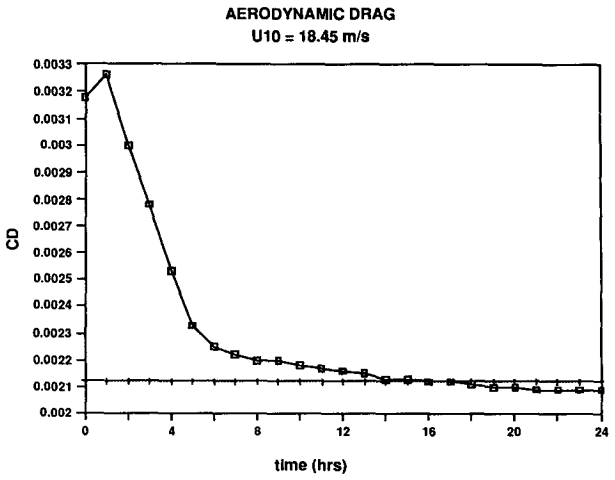

FIG. 6. Aerodynamic drag as a function of time for uncoupled model (+) and coupled model (□).

as in the uncoupled case. The results for the coupled run in Figs. 3, 4, and 5 are denoted by the square (□) symbol. We infer from these figures that coupling has some impact on the results for wave height and wave stress. The Phillips constant α_p behaves in a satisfactory manner and obtains, after 24 h, the limiting value $\alpha_p = 0.008$. The impact of the sea state on the aerodynamic drag is shown in Fig. 6. Evidently, the reference run shows no dependence of the drag on duration, whereas the coupled run gives a considerable variation in drag with time, because drag depends on the sea state through the wave-induced stress τ_w (the time dependence of which is given in Fig. 5). To conclude the presentation of the results of this coupled experiment, we show in Fig. 7 the evolution in time of the frequency spectrum. The combination of a stronger dissipation at high frequencies and a stronger interaction between wind and waves for young wind sea gives a more pronounced overshoot when compared with standard WAM model results (cf., WAMDI Group 1988).

Next, results of the coupled ocean-wave–atmospheric model for a turning wind field are shown. Using a single gridpoint version, after 6 hours we turn the wind by 90°. The corresponding evolution of the drag coefficient in time is shown in Fig. 8. The significant reduction in drag at $T = 7$ h and the subsequent increase is of interest to note. Also, the second maximum in drag is lower than the first maximum. These features may be explained as follows. As soon as the wind turns, new wind sea is generated in the new wind direction. In comparison with the case of absent old wind sea, the buildup of new wind sea is slowed down by the very presence of old wind sea (swell) because the quasi-linear dissipation [Eq. (38)] is much larger. This explains both the sudden drop at $T = 7$ h and the lower secondary maximum in drag. It should be realized that if a so-called second-generation wave model (e.g., Janssen et al. 1983) had been used to calculate the wave stress, the delicate behavior of the drag would not have been found. In such an event the second maximum would be as large as the first one.

We finally implemented the coupled code on a Convex minisuper, running this coupled code on the limited area of the North Sea and the Norwegian Sea (Janssen et al. 1983) with a resolution of 75 km. The source term integration time step was 15 minutes, whereas the advection time step was chosen as 30 min in order to meet the stability criterion for the first-order upwinding scheme. The wind fields used were analyses produced by the KNMI atmospheric model, implemented for the North Atlantic and western Europe (Stoffelen et al. 1990). The stress in the surface layer, including the wave-induced stress, was determined by

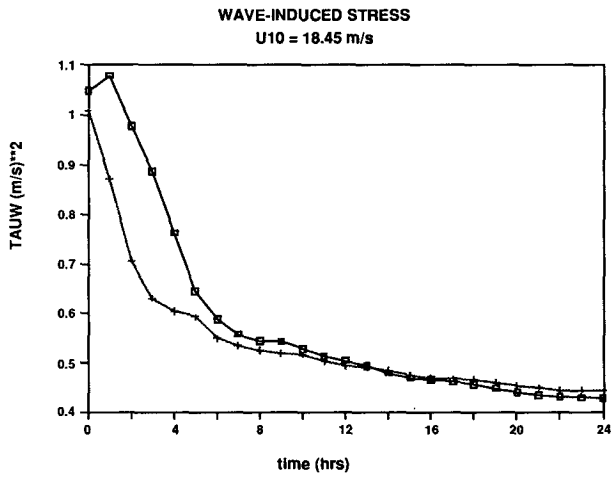

FIG. 5. Wave-induced stress as a function of time. Symbols: (+) uncoupled model, (□) coupled model.

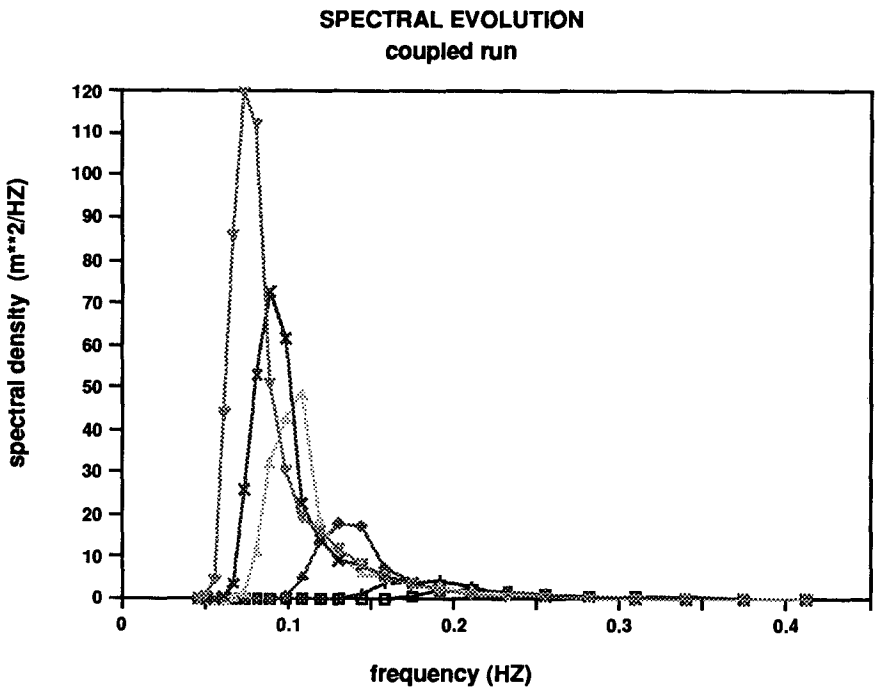

FIG. 7. Evolution of one-dimensional frequency spectrum with time. (□) T = 1 h, (+) T = 2 h, (◇) T = 4 h, (△) T = 8 h, (×) T = 12 h, and (▽) T = 24 h.

Eq. (23). A one-day run was performed with the coupled code from 89121612 until 89121712; Fig. 9 gives a plot of drag coefficient C_D wind speed U_{10} for the entire limited sea area. In agreement with the observations of Donelan (1982), a realistic scatter in the relation of drag versus wind speed is found. Evidently, this scatter may be attributed to the effect of waves on the stress in the surface layer.

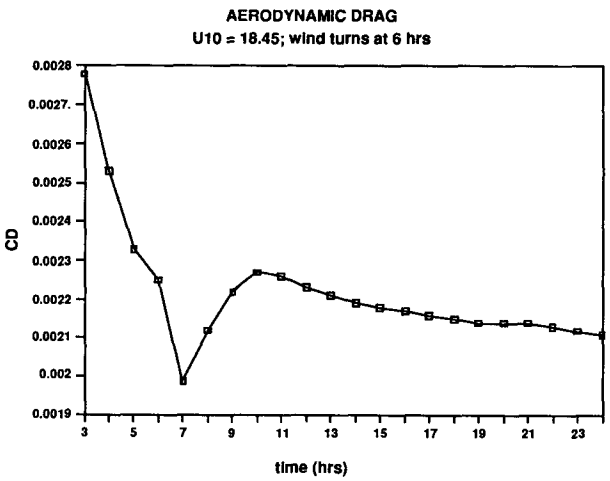

FIG. 8. Evolution of drag coefficient with time for turning wind field case. Wind turns after 6 h.

It should be noted that the data was stratified for the drag by means of the wave age c_p/u_* and that we used different symbols in Fig. 9 for different classes of wave age. However, no clear stratification according to wave age is present in Fig. 9. The reason for this is that the wave stress is determined by the high-frequency part of the spectrum and that, in mixed wind sea and swell cases, no definite relation between wave age and the high-frequency part of the spectrum exists. A similar conclusion may be drawn from the observations of Donelan. Inspecting the expression for the roughness length z_2 [Eq. (22)], it is immediately obvious that a labeling of the data by means of the ratio τ_w/τ would be much more effective in stratifying the data. This is indeed confirmed by Fig. 10 where the label τ_w/τ is used. However, in the field it might be difficult to determine the wave-induced stress τ_w so that in practice the usefulness of τ_w/τ remains to be seen.

Thus far we have assumed that the wind fields as produced by the atmospheric model are correct. This may be a reasonable assumption for analyzed fields (provided there are sufficient wind speed data for assimilation), but this assumption does not seem to be justified in forecasting mode since, especially for young wind sea, increased stresses due to ocean waves may result in an extra slowing down of the wind field. Convincing evidence of this problem can only be produced by developing a coupled atmosphere–wave model. Work in this direction is under way, and we hope to

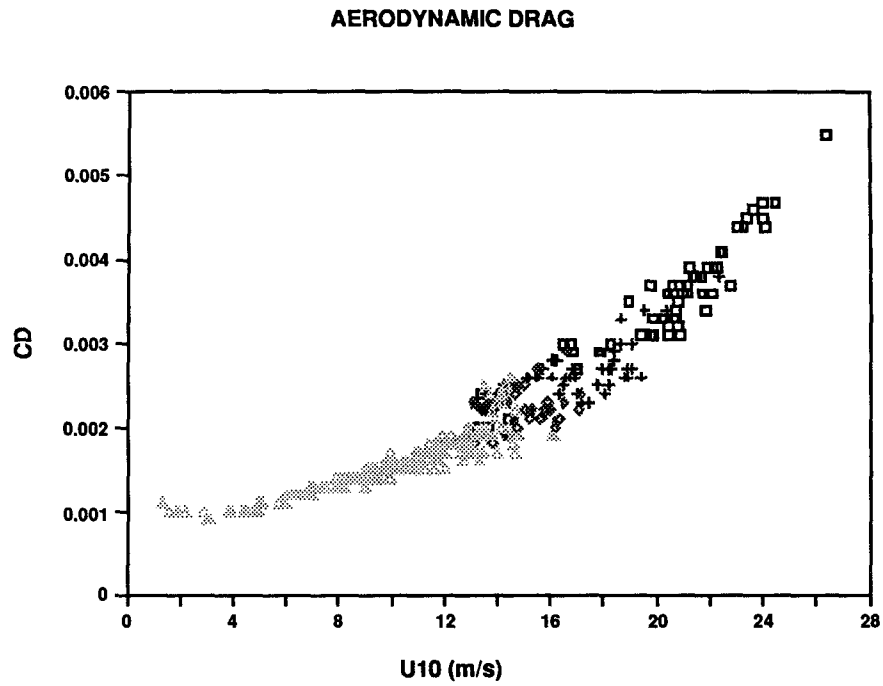

FIG. 9. Drag coefficient as a function of wind speed U_{10} for North Sea hindcast at DTG: 89 1217:12. Results are labeled according to wave age c_p/u_*. Symbols: (□) $10 < c_p/u_* < 15$, (+) $15 < c_p/u_* < 20$, (◇) $20 < c_p/u_* < 25$, (△) $c_p/u_* > 25$.

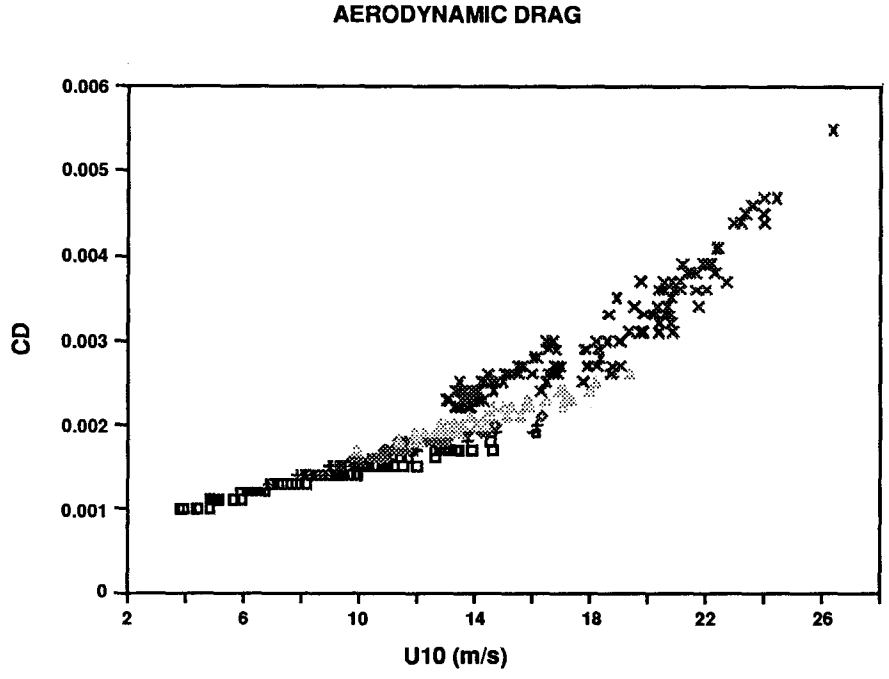

FIG. 10. As in Fig. 9, except that now results are labeled according to the ratio τ_w/τ. Symbols: (□) $\tau_w/\tau < 0.6$, (+) $0.6 < \tau_w/\tau < 0.7$, (◇) $0.7 < \tau_w/\tau < 0.8$, (△) $0.8 < \tau_w/\tau < 0.9$, (×) $0.9 < \tau_w/\tau < 1.0$.

report in the near future on the possible impact of ocean waves on the long-term evolution of the weather.

4. Summary of conclusions

In this paper we have discussed the effect of wind-generated gravity waves on the airflow. Especially for young wind sea, when the wave-induced stress is a large fraction of the total stress in the surface layer, the waves will affect the wind profile and thereby partly reduce the momentum transfer from wind to waves.

For a given wave spectrum, steady-state calculations of the wind profile over ocean waves show that for young wind sea most of the stress is determined by momentum transfer from wind to waves (i.e., a strong coupling), whereas for old sea there is hardly any coupling. A strong wave-age dependence of aerodynamic drag is therefore found to be in agreement with the observations. In this paper, we parameterized the effect of waves on wind by assuming a logarithmic wind profile with a roughness that depends on the wave-induced stress. As a consequence, the growth rate of waves by wind depends on the sea state as well.

Next, we allowed the wave spectrum to evolve according to the dynamics of the energy balance equation. To that end we coupled the WAM model to a simple, steady-state surface-layer model. Results of the coupled model show that a satisfactory behavior of the wave-induced stress is found provided the dissipation source term in the wave model is modified. Coupling has a significant impact on results for the stress in the surface layer. Also, the combination of modified dissipation and stronger interaction for young wind sea gives, when compared with the present version of WAM, a more realistic overshoot in the evolution of the wave spectrum. From our North Sea hindcast we see that a classification of the sea state by means of the wave age parameter c_p/u_* is too schematic. Although for pure wind sea a definite relation between wave age and the high-frequency part of the spectrum does exist, no definite relation exists in the case of mixed wind sea and swell. Therefore, stratification of the drag over ocean waves by means of c_p/u_* has its limitations. On the other hand, a labeling by means of the ratio τ_w/τ seems to be much more effective.

Although quasi-linear theory of wind-wave generation already gives realistic results, there are some problems that need further investigation. First, it should be realized that the Miles instability mechanism disregards the effect of air turbulence on the wave-induced air velocity and pressure. Air turbulence may be important for high-frequency waves (e.g., see Jacobs 1987). Second, we parameterized the momentum loss of air flow to the short gravity–capillary waves by introducing the Charnock relation for the roughness length. A more elegant approach is, perhaps, to determine this momentum loss by calculating the gain of momentum of these high-frequency waves. Presently, however, neither a reliable spectral shape nor a reliable expression for wind input (e.g., the nature of instability) to these short waves is known.

Acknowledgments. Stimulating discussion with Gerbrand J. Komen is gratefully acknowledged. Support by Gerrit Burgers and Gao Quanduo in implementing the coupled code on the KNMI Convex computer is very much appreciated.

REFERENCES

Banner, M. L., 1990: Equilibrium spectra of wind waves. *J. Phys. Oceanogr.*, **20,** 966–984.

Birch, K. G., and J. A. Ewing, 1986: Observations of wind waves on a reservoir. IOS-Rep. No. 234, 37 pp.

Charnock, H., 1955: Wind stress on a water surface. *Quart. J. Roy. Meteor. Soc.*, **81,** 639–640.

Cubasch, U., 1989: A global coupled atmosphere–ocean model. *Phil. Trans. R. Soc. London, A,* **329,** 263–273.

Donelan, M., 1982: The dependence of the aerodynamic drag coefficient on wave parameters. *Proc. of the First Int. Conf. on Meteorology and Air–Sea Interactions of the Coastal Zone,* The Hague, The Netherlands, Amer. Meteor. Soc., 381–387.

Forristal, G. Z., 1981: Measurements of a saturated range in ocean wave spectra. *J. Geophys. Res.*, **86,** 8075–8084.

Hasselmann, K., T. P. Barnett, E. Bouws, H. Carlson, D. E. Cartwright, K. Enke, J. A. Ewing, H. Gienapp, D. E. Hasselmann, A. Meerburg, P. Müller, D. J. Olbers, K. Richter, W. Swell and H. Walden, 1973: Measurements of wind wave-growth and swell decay during the Joint North Sea Wave Project (JONSWAP). *Dtsch. Hydrogr. Z.,* Suppl. A, **80,**(12).

——, 1974: On the spectral dissipation of ocean waves due to white-capping. *Bound.-Layer Meteor.* **6,** 107–127.

Hasselmann, S., K. Hasselmann, J. H. Allender and T. P. Barnett, 1985: Computations and parameterizations of the nonlinear energy transfer in a gravity-wave spectrum. Part II. Parameterizations of the nonlinear transfer for application in wave models. *J. Phys. Oceanogr.*, **15,** 1378–1391.

Jacobs, S. J., 1987: An asymptotic theory for the turbulent flow over a progressive water wave. *J. Fluid Mech.*, **174,** 69–80.

——, 1989: Effective roughness length for turbulent flow over a wavy surface. *J. Phys. Oceanogr.*, **19,** 998–1010.

Janssen, P. A. E. M., 1982: Quasi-linear approximation for the spectrum of wind-generated water waves. *J. Fluid Mech.*, **117,** 493–506.

——, 1987: The initial evolution of gravity-capillary waves. *J. Fluid Mech.*, **184,** 581–597.

——, 1989: Wave-induced stress and the drag of airflow over sea waves. *J. Phys. Oceanogr.*, **19,** 745–754.

——, P. Lionello and L. Zambresky, 1989: On the interaction of wind and waves. *Phil. Trans. R. Soc. London,* **A329,** 289–301.

——, G. J. Komen and W. J. P. de Voogt, 1984: An operational coupled hybrid wave prediction model. *J. Geophys. Res.*, **89,** 3635–3654.

Komen, G. J., 1985: Energy and momentum fluxes through the sea surface. *Dynamics of the Ocean Surface Mixed Layer,* P. Müller and D. Henderson, Eds., *Proceedings 'Aha Huliko'a,* Hawaii Institute of Geophysics, special publications, 1987, 207–217.

Maat, N., C. Kraan and W. A. Oost, 1991: The roughness of wind waves. *Bound.-Layer Meteor.*, **54,** 89–103.

Makin, V. K., 1988: Numerical results on the structure of the sea wave-induced pressure field in atmosphere. *Morskoy Gidnofizichesky Zhurnal,* No. 2, 50–54.

Maier-Reimer, E., K. Hasselmann, D. Olbers and J. Willebrand, 1982: An ocean circulation model for climate studies. Tech. Rep. M.P.I. für Meteorologie Hamburg.

Miles, J. W., 1957: On the generation of surface waves by shear flows. *J. Fluid Mech.*, **3,** 185–204.

——, 1965: A note on the interaction between surface waves and wind profiles. *J. Fluid Mech.*, **22,** 823–827.

Nikolayeva, Y. L., and L. S. Tsimring, 1986: Kinetic model of the wind generation of waves by a turbulent wind. *Izv. Acad. Sci. USSR, Atmos. Ocean, Phys.*, **22,** 102–107.

Plant, W. J., 1982: A relationship between wind stress and wave slope. *J. Geophys. Res.*, **88,** 1961–1967.

——, and J. W. Wright, 1977: Growth and equilibrium of short gravity waves in a wind wave tank. *J. Fluid Mech.*, **82,** 767–793.

Sausen, R., K. Barthels and K. Hasselmann, 1988: Coupled ocean-atmosphere models with flux correction. *Climate Dyn.*, **2,** 154–163.

Snyder, R. L., F. W. Dobson, J. A. Elliot and R. B. Long, 1981: Array measurements of atmospheric pressure fluctuations above surface gravity waves. *J. Fluid Mech.*, **102,** 1–59.

Stoffelen, A. C. M., G. Cats, L. M. Hafkenscheid and A. P. M. Baede, 1990: Impact of SASS wind data on analyses and forecasts of a finemesh limited area model. BCRS-Rep. No. 89–38, 80 pp.

The WAMDI Group (S. Hasselmann, K. Hasselmann, E. Bauer, P. A. E. M. Janssen, G. J. Komen, L. Bertotti, P. Lionello, A. Guillaume, V. C. Cardone, J. A. Greenwood, M. Reistad, L. Zambresky and J. A. Ewing), 1988: The WAM model—a third generation ocean wave prediction model. *J. Phys. Oceanogr.*, **18,** 1775–1810.